Metallomics, 14, 2022, mfac036
https://doi.org/10.1093/mtomcs/mfac036
Advance access publication date: 1 June 2022
Paper

Bioconjugated chelates based on (methylpyridinyl)tacn: synthesis, ^{64}Cu labeling and *in vitro* evaluation for prostate cancer targeting

Axia Marlin[1], Ina Hierlmeier[2], Amaury Guillou[1], Mark Bartholomä[2], Raphaël Tripier[1,*] and Véronique Patinec[1,*]

[1]University of Brest, UMR-CNRS 6521 CEMCA, 6 Avenue Victor le Gorgeu, 29238 Brest, France. and [2]Department of Nuclear Medicine, Saarland University—Medical Center, Kirrbergerstrasse, 66421 Homburg, Germany
*Correspondence: Univ Brest, UMR-CNRS 6521 CEMCA, 6 Avenue Victor le Gorgeu, 29238 Brest, France. E-mails: raphael.tripier@univ-brest.fr; veronique.patinec@univ-brest.fr

Abstract

Three new bifunctional copper chelators based on the 1,4,7-triazacyclononane (tacn) platform have been synthesized and conjugated to peptides. The first one is constituted of the tacn with two methylpyridinyl and one methylthiazolyl carboxylic acid pendant arms, while, in the second and third ones, the macrocycle is functionalized by three methylpyridinyl groups, with an additional hexynoic acid chain on a carbon of one or two pyridine rings. These three bifunctional chelators have been conjugated to the antagonist DPhe-Gln-Trp-Ala-Val-Gly-His-Sta-Leu-NH_2 peptide for targeting the gastrin-releasing peptide receptor, which is overexpressed in prostate cancer. The resulting monomeric bioconjugates have shown their efficiency to be radiolabeled with β^+ emitter ^{64}Cu, and the hydrophilicity and PC-3 cell internalization properties of these radiolabeled conjugates have been studied. PC-3 cell binding affinity of mono- and dimeric metal-free and ^{nat}Cu metallated conjugates have been evaluated by IC_{50} measurements. The results demonstrate the potential of these methylpyridinyl tacn derivatives for radiopharmaceutical applications.

Keywords: 1,4,7-triazacyclononane, bioconjugation, bivalency, ^{64}Cu, radiolabeling, GRP-r

Graphical abstract

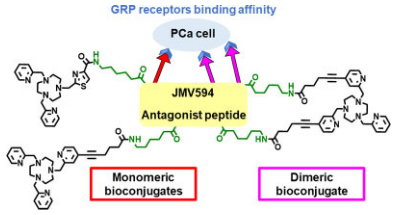

Three novel tacn-based monomeric or dimeric bifunctional ligands were conjugated to the antagonist peptide JMV594 for GRP-r targeting for radiopharmaceutical applications.

Introduction

Positron emission tomography (PET) is an imaging technique in nuclear medicine that underwent continuing progress for the last 20 yr resulting in higher accessibility of PET devices for diagnosis in healthcare facilities. Research in this field has in parallel known a growing interest thanks to the development of cyclotrons and generators affording easier and larger production of suitable PET imaging radiometals that release a β^+ positron with interesting half-life and energy.[1–3] Copper-64 with a half-life of 12.7 h and a positron energy of 656 keV (19%) presents attractive properties for PET imaging. Additionally, it forms an interesting theranostic pair with its β^--emitting congener copper-67 ($t_{1/2}$ = 61.8 h; β^- 141 keV; 100%) that exhibits potential for therapeutic applications.[4] For PET applications, radiopharmaceuticals based on radiometals generally require a bifunctional chelator for coordinating the radiometal (first functionality) that is covalently linked through a spacer (second functionality) to a biological targeting moiety. In case of cancer, peptides are well established as biovectors to target selective receptors expressed on the surface of cancer cells. In prostate cancer (PCa), which is one of the most prevalent cancer types in men, the gastrin-releasing peptide receptor (GRP-r) is overexpressed, while being absent in surrounding healthy tissues making the GRP-r an excellent target for tumor-specific imaging.[5] GRP possesses a sequence similar to bombesin (BBN), a 14 amino acid peptide isolated first from a fire-bellied toad skin (*Bombina bombina*).[6] Human GRP is constituted of 27 amino acids among which 7, in common with BBN, are responsible for the high affinity for GRP-r.[7] Antagonist BBN-like peptides that display no or low internalization in cells have shown higher efficiency in targeting receptors with less side

Received: March 15, 2022. **Accepted:** May 2, 2022

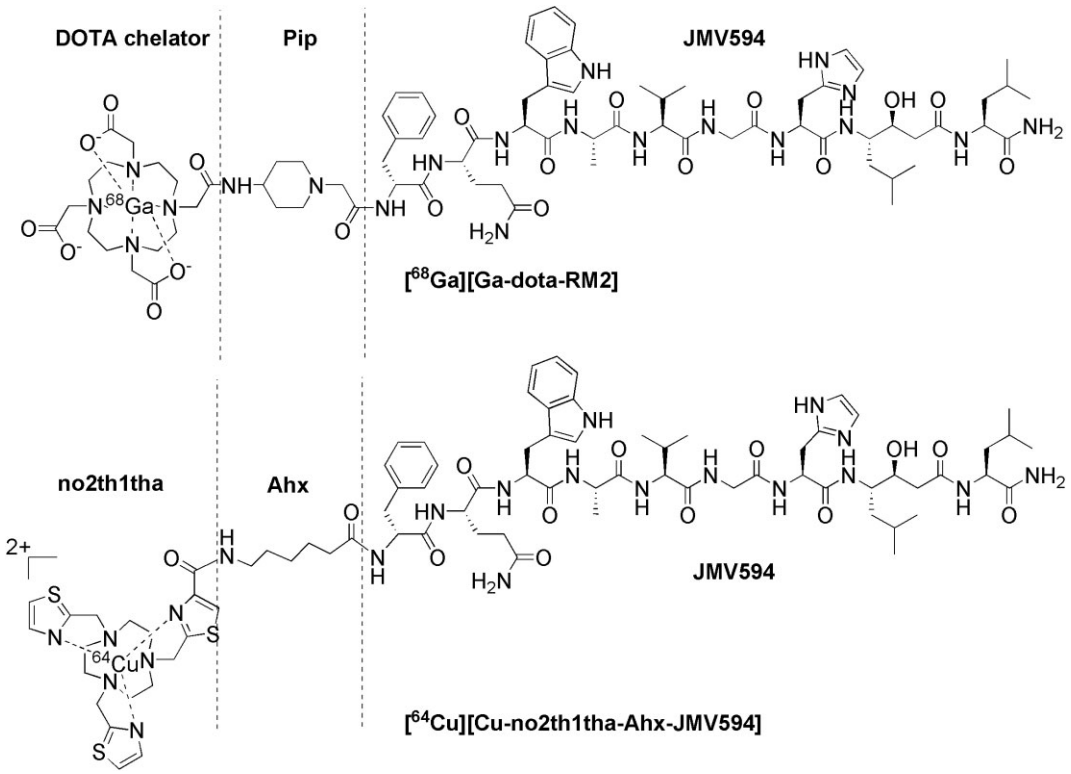

Fig. 1 [^{68}Ga][Ga-dota-RM2] and [^{64}Cu]Cu-no2th1tha-Ahx-JMV594] radioconjugates.

effects than internalizing agonist analogues, giving rise to their large investigation as biological vectors in radiopharmaceuticals for PCa imaging.[8] One of the widely used antagonist peptides in radiopharmaceuticals is the statine-based JMV594 (DPhe-Gln-Trp-Ala-Val-Gly-His-Sta-Leu-NH_2).[9,10] Moreover, different studies have also discussed the effect of the polyvalency of peptide homodimers on the affinity for GRP-r. Multivalent interactions are indeed suggested to increase the affinity strength between ligands and receptors depending on the size, shape, and length of the resulting framework.[11] In case of peptide homodimers that are expected to link to two receptors simultaneously, the spacer length between the two peptides firstly and the receptors density secondly are two important parameters that impact the effect of bivalency.[12,13] Results of BBN-like dimers compared to monomers are heterogeneous, showing no differences in some cases, while others show superior cellular uptake.[14–17] Indeed, the dimer ^{68}Ga-HBED-CC-[PEG_2-(4-amino-1-carboxymethylpiperidine)-JMV594]$_2$ (PEG: polyethylene glycol) has recently exhibited higher cell binding than the corresponding radiolabeled monomer.[18]

The antagonistic monomer [^{68}Ga][Ga-dota-RM2] (dota: 1,4,7,10-tetraazacyclododecane-1,4,7,10-tetraacetic acid), based on the dota-scaffold as chelating moiety and the JMV594 peptide vector linked through the 4-amino-1-carboxymethylpiperidine entity as spacer, is currently in clinical studies for PCa imaging (Fig. 1).[19–21] In contrast to neutrally charged spacers such as PEG or Ahx (6-aminohexanoic acid), the methylpiperidine group is protonated at physiological pH inducing a positive charge at the N-terminus of the peptide sequence, which had been suggested to improve the binding affinity to GRP-r.[20,22,23]

The 1,4,7-triazacyclononane (tacn) derivatives are well suited for copper(II) complexation explaining their great part in new tacn-based ^{64}Cu radiolabeling radiopharmaceuticals for PET imaging. For instance, bifunctional nota (tacn-1,4,7-triacetic acid) derivatives were used in synthesis of promising bioconjugates involving an Ahx spacer and the BBN-like JMV594 peptide.[23] In a previous work, we demonstrated that tacn derivatives with methylthiazolyl or methylpyridinyl pendant arms, Hno2th1tha and no3py, are good copper(II)-complexing agents and better chelators than nota in terms of thermodynamic stability, kinetic stability, and redox reversibility properties of the Cu(II) complexes, which are essential parameters for potential *in vivo* applications.[24,25] Hno2th1tha was then easily conjugated to the JMV594 peptide through an Ahx spacer and the resulting bioconjugate was efficiently radiolabeled with ^{64}Cu to form [^{64}Cu][Cu-no2th1tha-Ahx-JMV594] (Fig. 1) with a (+2) charge at the N-terminus induced by the positively charged $[Cu(no2th1tha)]^{2+}$ complex. This conjugate exhibited interesting biological affinities for PCa cells.[26] A bifunctional no3py derivative was also synthesized by introducing a carboxylic acid function on a carbon atom of a pyridine core, giving the Hno2py1pa ligand (Fig. 2).[27] This Hno2py1pa chelator exhibited efficient ^{64}Cu radiolabeling. Nevertheless, its conjugation to peptidic vector through the carboxylic function remained unsuccessful, bringing us to develop other alternatives.

In this work, we describe the synthesis of two new tacn-based bifunctional chelators with methylpyridinyl pendant arms Hno2py1tha and no3pyCOOK, their bioconjugation to the Ahx-JMV594 antagonist peptide, and the ^{64}Cu radiolabeling, lipophilic character, and cell internalization assays studies with the two resulting conjugates distinguished by the bifunctional nature. A third new dimeric chelator no3py$(COOK)_2$ synthesis is also described and the last part is devoted to the study of bivalency contribution to the binding affinity for GRP-r of the corresponding peptidic homodimer bioconjugate obtained by the introduction of Ahx-JMV594 peptide on two py groups of no3py.

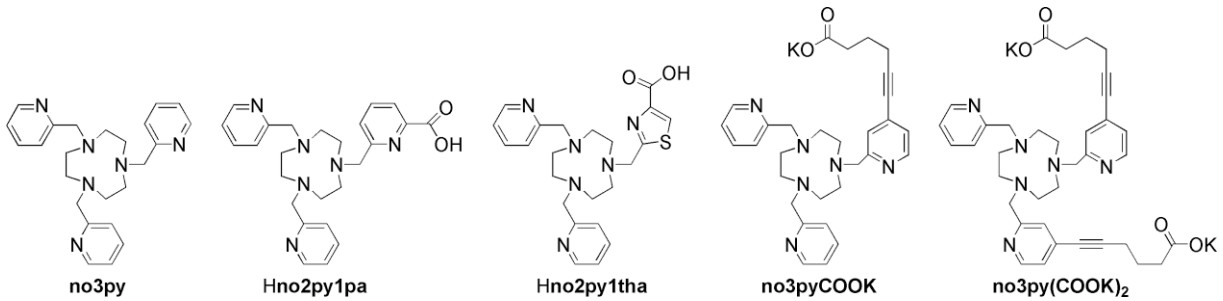

Fig. 2 Ligands discussed in this work.

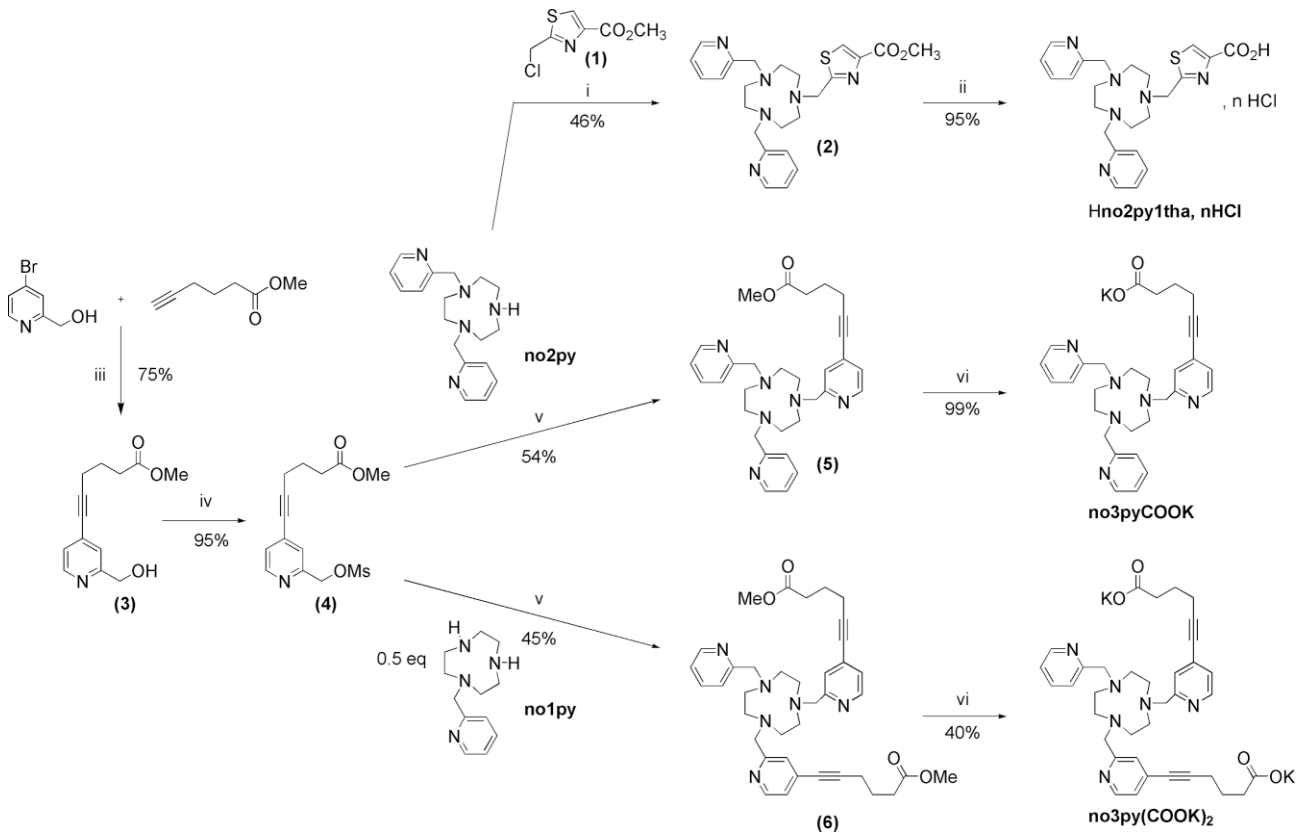

Scheme 1. Synthesis of the bioconjugable triazamacrocyclic chelators Hno2py1tha, no3pyCOOK and no3py(COOK)$_2$ (i) K_2CO_3, CH_3CN, 3d, rt; (ii) 6M HCl, reflux, 12 h; (iii) $[Pd(PPh_3)_2]Cl_2$, CuI, THF/Et_3N, 55°C, 18h; (iv) MsCl, Et_3N, CH_2Cl_2, 4h, 25°C; (v) K_2CO_3, CH_3CN, 4d, rt; and (vi) 1M KOH/THF, 55°C, 18h, purification by semi-preparative HPLC.

Results and discussion

Bioconjugable ligands synthesis

For subsequent BBN conjugation of methylpyridinyl tacn, we have chosen the same approach that was previously used for the synthesis of no2th1tha-Ahx-JMV594, by introducing a methylthiazolyl carboxylic acid (tha) arm instead of a pyridine group (py), giving the new bifunctional ligand Hno2py1tha (Fig. 2). Synthesis of this chelator was based on the no2py platform as starting material that was reacted with 2-(chloromethyl)thiazolyl-4-carboxylic acid methyl ester (1) in CH_3CN to produce the intermediate (2) in 46% yield after purification.[27–29,30] Acidic hydrolysis of (2) in 6M HCl gave quantitatively the bifunctional Hno2py1tha as hydrochloride salt (Scheme 1). In parallel, we have undertaken to implant the Ahx-JMV594 BBN conjugation via an additional functionality on one pyridine group of no3py in order to compare the properties of these two new resulting bioconjugates. The synthesis of the bioconjugable version of the no3py chelator can either be achieved through C-functionalization of a CH_2 carbon of the tacn macrocycle or of the pendant arms as it has already been described by others.[31–35] These options require nevertheless reconsidering the fastidious whole macrocycle synthesis in the first case and would imply anyway to take the formation of stereoisomers into consideration. A C-heterocycle ring functionalization methodology was previously used to obtain the bifunctional Hno2th1tha tacn derivative by incorporating a carboxylic acid function on a carbon atom of one thiazole aromatic ring.[26] Introduction of an additional function on a pyridine moiety was therefore chosen in order to obtain bifunctional derivatives of no3py. Sonogashira coupling is known to allow the substitution of an aryl halide with terminal alkyne using palladium and copper catalysis. Consequently, synthesis of a pyridine-based bifunctional arm was engaged by reacting (4-bromo-pyridin-2-yl)methanol with methylhex-5-ynoate to perform the Sonogashira coupling

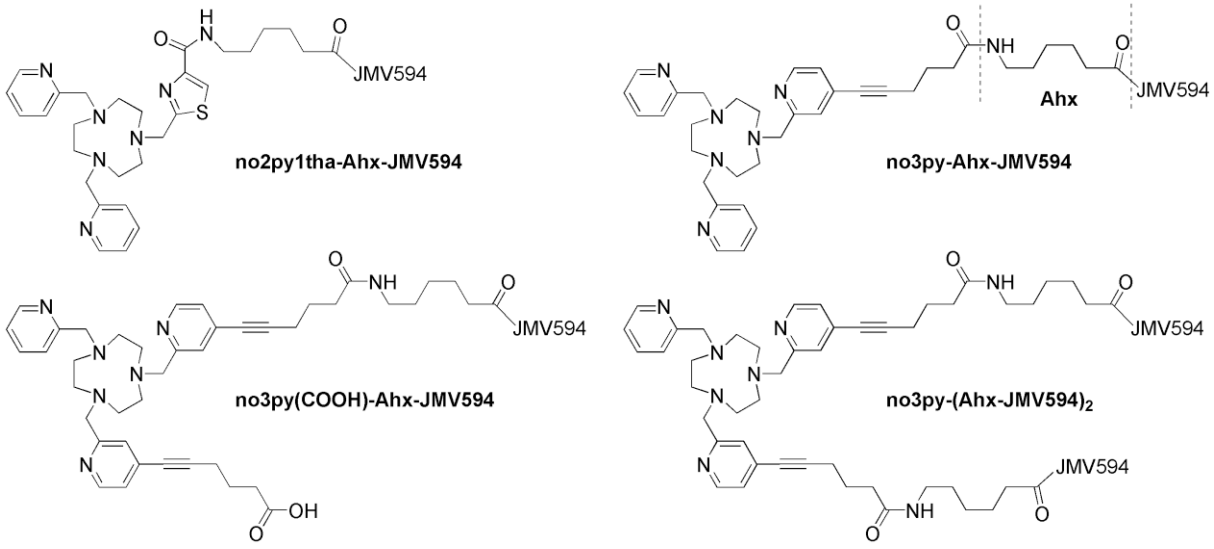

Fig. 3 no3py-based Ahx-JMV594 conjugates discussed in this paper.

and obtain compound (3) after purification by silica gel column chromatography. The bifunctional arm (4) was finally synthesized after conversion of the hydroxyl group into its mesylate in 95% yield by reaction with methanesulfonyl chloride without purification (Scheme 1). The synthesis strategy of bifunctional no3py was therefore based on the addition of one bioconjugable pyridinyl arm (4) to the corresponding tacn derivative, namely no2py, in order to obtain no3pyCOOK (Scheme 1). Saponification of intermediate (5) with KOH in tetrahydrofuran (THF) gave no3pyCOOK in 25% overall yield in seven reaction steps from commercial tacn, including the no2py platform synthesis.[27–29]

The same methodology was used for synthesis of the dimeric bifunctional ligand no3py$(COOK)_2$, starting from the already known no1py skeleton, which was introduced in half quantity in CH_3CN together with the reactive arm (4).[36] The diester (6) was obtained after consumption of (4) monitored by Thin-Layer Chromatography (TLC), in 45% yield after purification by neutral alumina chromatography column. Hydrolysis of the ester functions was undertaken by KOH in THF during an optimized time of 9 h in order to minimize the arm degradation. The no3py$(COOK)_2$ was isolated with 40% yield after final purification by using semi-preparative High Performance Liquid Chromatography (HPLC). Full characterization data of these different intermediates and azamacrocyclic chelates are presented in the supplementary material (Supplementary Figs. S1–S14).

Bioconjugate and metallopeptide synthesis

JMV594 was conjugated to the three bifunctional chelators by peptidic coupling in order to explore their applicability for ^{64}Cu-based radiopharmaceuticals targeting GRP-r as a model for PCa. As previously used with Hno2th1tha, Ahx was employed as spacer to connect our bifunctional tacn platforms to the JMV594 antagonist peptide. Conjugation of Hno2py1tha was carried out as previously described for the tha pendant arm by reacting the carboxylic acid group with the NH_2-terminus of the peptide linked to a Rink amide resin, after transformation of the tha acidic function into an active ester form with 1-[bis(dimethylamino)methylene]1*H*-1,2,3-triazolo[4,5-*b*]pyridinium-3-oxide hexafluorophosphate (HATU).[26] After cleavage of the resin using trifluoroacetic acid (TFA)/water (H_2O)/triisopropylsilane (TIS) mixture, the final bioconjugate no2py1tha-Ahx-JMV594 was obtained in 10% yield after semi-preparative reversed-phase HPLC (RP-HPLC) purification (Fig. 3, Supplementary Figs. S15 and S16).

For the second monomeric no3py-based bioconjugate synthesis, the carboxylate group of no3pyCOOK was first activated by reaction with benzotriazol-1-yl-oxy-tris-pyrrolidino-phosphonium hexafluorophosphate (PyBOP) and 1-hydroxybenzotriazole (HOBt) coupling agents in the presence of N,N-Diisopropylethylamine (DIPEA) as a base, prior to coupling with the peptide Ahx-JMV594 in solution. The conjugate no3py-Ahx-JMV594 was obtained in 25% yield after RP-HPLC purification (Supplementary Figs. S17 and S18).

In the case of no3py$(COOK)_2$, the peptidic coupling conditions in N,N-dimethylformamide (DMF) solution using PyBOP and HOBt only produced the undesired monomer no3py(COOH)-Ahx-JMV594 (Fig. 3). The peptidic dimeric bioconjugate was therefore synthesized by solid-phase synthesis under similar conditions as used for no2py1tha-Ahx-JMV594. After cleavage from the resin, the final bioconjugate no3py-$(Ahx\text{-}JMV594)_2$ was obtained in 20% yield after RP-HPLC purification (Fig. 3, Supplementary Figs. S19 and S20).

The three bioconjugates no2py1tha-Ahx-JMV594, no3py-Ahx-JMV594, and no3py-$(Ahx\text{-}JMV594)_2$ were reacted with aqueous solutions of $CuCl_2$ to provide the corresponding Cu(II) metalloconjugates that were intended for biological investigations. The HPLC analysis exhibited purity higher than 99% for the three bioconjugates and the corresponding metallopeptides (Supplementary Figs. S15–S26). HPLC analysis of no3py-$(Ahx\text{-}JMV594)_2$ revealed two equal intensity signals, which we attribute to the presence of two conformers due to interactions between the two peptidic chains of the bioconjugate (Supplementary Fig. S19). This hypothesis was supported by the subsequent generation of a single peak in the HPLC analysis of the corresponding complex [Cu(no3py-$(Ahx\text{-}JMV594)_2$)] (Supplementary Fig. S25).

No2py1tha-Ahx-JMV594 and no3py-Ahx-JMV594 bioconjugates study

Radiolabeling

Radiolabeling was performed by reacting the bioconjugates no3py-Ahx-JMV594 and no2py1tha-Ahx-JMV594 with [^{64}Cu]$CuCl_2$

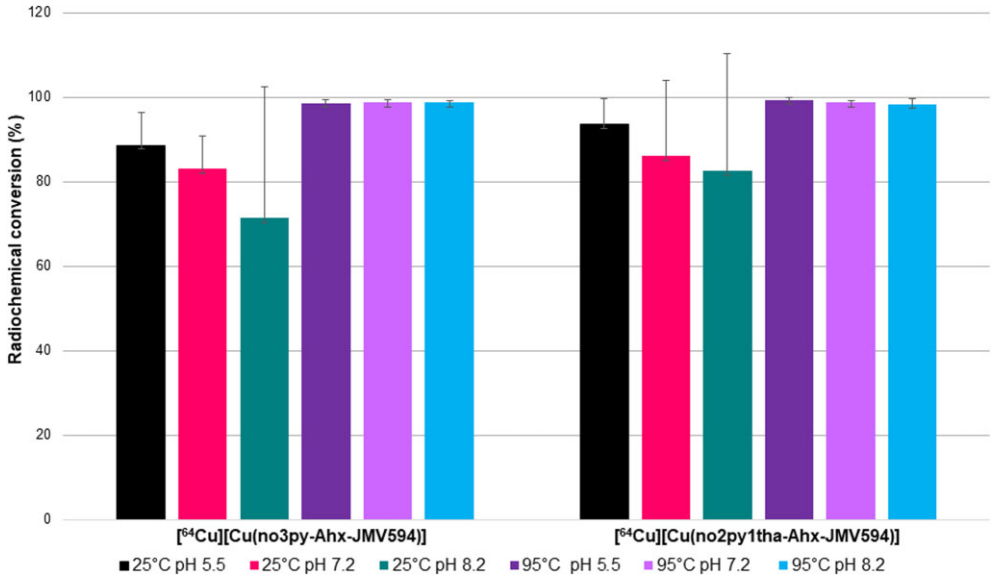

Fig. 4 Radiochemical conversion of radioconjugates depending on pH and temperature.

Table 1 Comparison of the log*D* values of ^{64}Cu labeled bioconjugates

Conjugates	[^{64}Cu][Cu(dota-RM2)]	[^{64}Cu][Cu(no3py-Ahx-JMV594)]	[^{64}Cu][Cu(no2py1tha-Ahx-JMV594)]
Log*D*	−2.54 ± 0.04	−2.23 ± 0.01	−2.19 ± 0.01

at different pHs and temperatures to determine the optimal conditions for radiolabeling at 0.4 μmol L^{-1} (Fig. 4). Lower concentrations of bioconjugates were also tested for selected pH values and conditions. However, radiochemical conversions (RCCs) decreased at lower concentrations such that quantitative RCCs could not be obtained. The two conjugates no3py-Ahx-JMV594 and no2py1tha-Ahx-JMV594 were radiolabeled quantitatively (≥98%) at 95°C within 15 min at pH 5.5, 7.2, and 8.2 in molar activities of ∼20 MBq/nmol. At room temperature (25°C), the radiochemical yields slightly decreased for both conjugates in the range of ∼70–93% independently of the pH, aiming the same molar activity of ∼20 MBq/nmol. These experiments allowed selecting the optimized conditions of pH 5.5 during 5 min at 95°C for ^{64}Cu radiolabeling of the bioconjugates for the subsequent *in vitro* experiments. Radio-TLC and radio-HPLC of these radiolabeled conjugates are presented in Supplementary Figs. S27–S30.

Lipophilicity studies

The partition coefficients log$D_{oct/PBS}$ were determined to be −2.23 ± 0.01 and −2.19 ± 0.01 for the ^{64}Cu-labeled [^{64}Cu][Cu(no3py-Ahx-JMV594)] and [^{64}Cu][Cu(no2py1tha-Ahx-JMV594)], respectively (Table 1). Both radiolabeled conjugates are less hydrophilic than the ^{64}Cu-labeled dota-RM2, which displayed log*D* value of −2.54 ± 0.04 (Table 1). This observation can be attributed to different parameters among which the more hydrophobic feature of the pyridine moiety compared to the acetate groups of the chelating unit and the positively charged Pip versus the neutral Ahx spacer.

Cell internalization assays

Cell internalization was assessed in the GRP-r expressing PCa cell line PC-3 with the ^{64}Cu-radiolabeled bioconjugates at 37°C. At 1 h, the receptor-specific surface bound activity was 9.5 ± 0.2% for the [^{64}Cu][Cu(no3py-Ahx-JMV594)] and the internalized activity was 1.4 ± error% being in line with the antagonistic character of the JMV594 peptide. The internalized activity of [^{64}Cu][Cu(no2py1tha-Ahx-JMV594)] was 1.5 ± 0.7%, whereas the surface-bound activity was 8.8 ± 0.9%. The [^{64}Cu][Cu(dota-RM2)] showed a higher surface-bound fraction of 17.3 ± 0.6% and an internalized amount of 1.3 ± 0.1% (Fig. 5). The bioconjugates tested only differ in their respective metal chelates and spacer entities compared to dota-RM2. It is well accepted that the (radio)metal chelate comprising the (radio)metal and the chelator impact the biological properties of radiotracers as receptor affinity, biodistribution, among others. The use of different radiometals with one particular metal chelator may already result in varying receptor affinities and biodistribution profiles *in vivo* of a particular bioconjugate. The most studied conjugates in this respect are probably somatostatin analogs such as DOTATATE.[37] Our conjugates differ significantly from dota-RM2 in the size, shape, overall charge, and polarity of the radiometal chelate compared to dota. We therefore attribute the differences in biological properties to the mentioned parameters despite having an identical binding motif/peptide sequence.

Competitive cell binding affinity study with no3py-Ahx-JMV594 and no3py-(Ahx-JMV594)$_2$ dimer bioconjugates

The interesting results of the radiolabeling, lipophilicity, and cell internalization assays studies motivated us to investigate

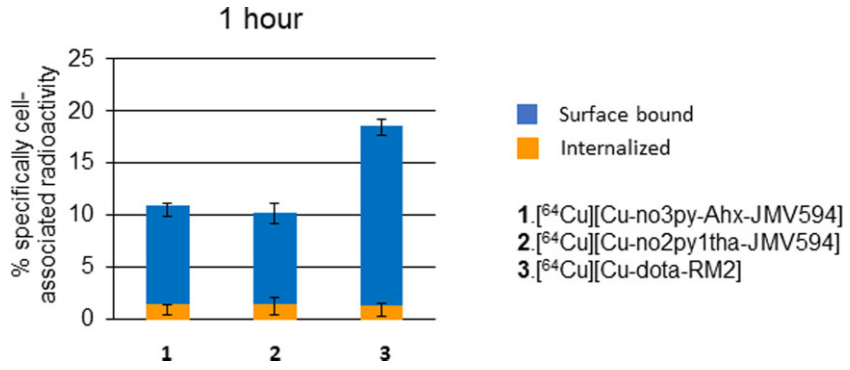

Fig. 5 Internalized and surface bound fractions of ^{64}Cu-radiolabeled bioconjugates expressed as percentage specifically cell-associated radioactivity in PC-3 cells at 37°C.

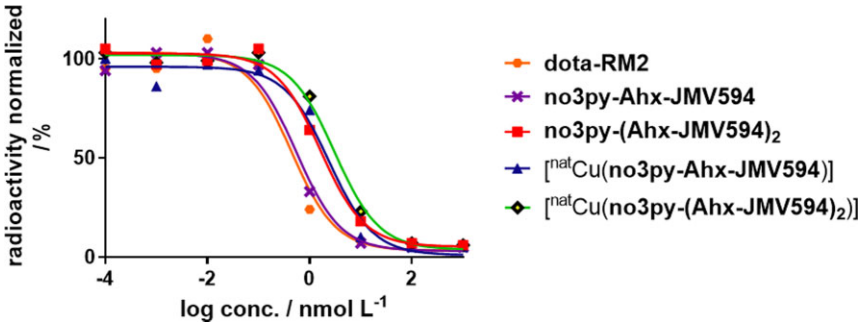

Fig. 6 IC_{50} curves as a function of conjugates and metallopeptides concentrations, obtained from *in vitro* competitive cell binding experiments on PC-3 cell line using [^{125}I]I-[Tyr$_4$]-BBN as the radioligand (experiments performed in triplicate).

Table 2. Comparison of the IC_{50} values of the studied conjugates and the metallopeptides (experiments performed in triplicate)

Conjugates	dota-RM2	no3py-Ahx-JMV594	[^{nat}Cu(no3py-Ahx-JMV594)]	no3py-(Ahx-JMV594)$_2$	[^{nat}Cu(no3py-(Ahx-JMV594)$_2$)]
IC_{50} (nM)	0.4 ± 0.2	0.5 ± 0.1	2.4 ± 0.2	1.6 ± 0.1	3.1 ± 0.1

the potential bivalency effect on the binding affinity of no3py derivatives for GRP-r. Multivalent interactions are advantageous compared to monovalent interactions due to increasing the binding affinity. Dimeric agonist BBN-like bioconjugates targeting GRP-r have shown some promising results as ^{64}Cu-nota-PEG$_2$-dimer of [D-Tyr^6, βAla^{11}, Thi^{13}, Nle^{14}] BBN (6–14) that showed prolonged tumor retention than the monomer analogue. This bivalency effect has also been demonstrated with ^{68}Ga radiolabeled homodimer antagonist HBED-CC-[PEG$_2$-Pip-JMV594]$_2$ with higher total cell binding than the corresponding monomer.[17,18]

Evaluation of the binding affinity can be achieved by competitive cell binding experiments on PC-3 cell line using [^{125}I]I-[Tyr$_4$]-BBN as the radioligand to afford corresponding IC_{50} values. Thus, the binding affinity of the monomeric no3py-Ahx-JMV594 and the dimeric no3py-(Ahx-JMV594)$_2$ bioconjugates and of their respective Cu(II) metallo-derivatives were determined in order to evaluate a potential bivalency effect. Dota-RM2 was used as the control (Fig. 6). The IC_{50} values for the monomeric no3py-Ahx-JMV594 and the dimeric bioconjugate no3py-(Ahx-JMV594)$_2$ were 0.5 ± 0.1 nM and 1.6 ± 0.1 nM, respectively (Table 2), showing no improved affinity for the dimeric form compared to the monomer derivative. This lower affinity of the dimeric form compared to the monomeric one is assumed to be related to steric hindrance caused by the second peptide in close proximity of the other peptide moiety making the distance between both peptides too short for allowing simultaneous bivalent binding and resulting in no improvement in binding affinity. Of interest, the binding affinity of no3py-Ahx-JMV594 was comparable to that of dota-RM2 with an IC_{50} value of 0.4 ± 0.2 nM making this conjugate a promising candidate for PCa targeting.

Metal complexation resulted in a slight decrease of the binding affinities of the metallopeptides [Cu(no3py-Ahx-JMV594)] and [Cu(no3py-(Ahx-JMV594)$_2$)] with IC_{50} values of 2.4 ± 0.2 nM and 3.1 ± 0.1 nM, respectively.

The N-terminus positive charge of bioconjugates has been suggested to improve the GRP-r binding affinity.[20,38] The metal-free conjugates no3py-Ahx-JMV594 and no3py-(Ahx-JMV594)$_2$ display a 1-fold-positive charge due to the protonated form of the no3py part at physiological pH, while dota-RM2 presents a neutral profile thanks to the (−1) charge of dota neutralized by the (+1) of the pip spacer.[24,39,40] The metalloconjugates [Cu(no3py-Ahx-JMV594)] and [Cu(no3py-(Ahx-JMV594)$_2$)] are characterized by the (+2) charge brought by the Cu^{2+} cation. The interesting low nanomolar IC_{50} values obtained for our four positively charged conjugates are nevertheless not consistent with an impact of positively charged N-terminus on the binding affinity of conjugates for GRP-r, as the +2 charged metalloconjugates gave higher IC_{50} results and dota-RM2 lower ones than non-metallated

bioconjugates. Other parameters such as chelator nature, hydrophilicity, and geometry have unambiguously predominant effects on the GRP-r binding affinity of these conjugates.

Conclusion

The present work focused on triazamacrocyclic chelator-based bioconjugates study implying the synthesis of new bifunctional chelator derivatives Hno2py1tha, no3pyCOOK, and no3py(COOK)$_2$. Their bioconjugation using Ahx spacer and JMV594 antagonist peptide were carried out to develop antagonist monomers and dimer. The linker hex-5-ynoic acid chain introduced on the pyridine group has shown its efficiency for conjugation and constitutes a new way for binding pyridinyl tacn derivatives to biological vectors.

The two monomeric metallated conjugates distinguished by the nature of the bifunctionality of the included chelate, presenting both a +2 overall charge exhibited no significant difference of behavior. The ^{64}Cu-radiolabeled monomeric conjugates were prepared in excellent radiochemical yields and expressed good hydrophilic properties. Cell internalization assays showed that they were mainly surface bound as expected for antagonist peptides.

The monomer no3py-Ahx-JMV594 exhibited very interesting PC-3 cells binding affinity with IC_{50} results in the same range as the standard dota-RM2 reference, showing clearly the potentialities of this new bioconjugate for PCa targeting and radiopharmaceutical applications. If IC_{50} values of the metal-free and Cu^{2+} dimer conjugates remain very interesting, no higher affinity has been revealed for PC-3 cells compared to the monomer no3py-Ahx-JMV594. An attractive point remains, however, in the possible refinement of the dimeric bioconjugate no3py-(Ahx-JMV594)$_2$ by designing longer spacer than Ahx, as observed for the previously discussed [^{64}Cu][Cu-nota-(PEG)$_2$-dimer] that exhibited higher binding affinity than the shorter analogue one PEG unity spacer [^{64}Cu][Cu-nota-(PEG)-dimer].[17]

Experimental section

Material and methods

Reagents were purchased from Acros Organics and from Aldrich Chemical Co. The tacn was purchased from CheMatech (Dijon, France). RM2 was obtained from ABX (Radeberg, Germany). [^{64}Cu]$CuCl_2$ was purchased from the Department of Preclinical Imaging and Radiopharmacy of the Eberhard Karls University (Tu¨bingen, Germany). [^{64}Cu]$CuCl_2$ was produced via the ^{64}Ni(p,n)^{64}Cu route.[41] Acetonitrile and tetrahydrofuran solvents were distilled before use. Coupling reagents PyBOP and HOBt were purchased from Carl Roth GmbH (Karlsruhe, Germany). Nuclear Magnetic Resonance (NMR) spectra were recorded at the "Services communs" of the University of Brest. ^{1}H et ^{13}C NMR spectra were recorded with Bruker Avance 500 (500 MHz), Bruker Avance 400 (400 MHz), or Bruker AMX-3 300 (300 MHz) spectrometers. Coupling constants are given in Hertz. HRMS analyses were carried on a HRMS Q-Tof MaXis instrument equipped with ElectroSpray Ionization (ESI), Atmospheric Pressure Chemical Ionization, Atmospheric Pressure PhotoIonization and nano-ESI sources (at the Institute of Organic and Analytic Chemistry—ICOA in Orléans).

Low-resolution mass spectrometry was performed on an Advion expression CMS spectrometer (Ithaca, NY, USA). All instruments measuring radioactivity were calibrated and maintained in accordance with previously reported routine quality-control procedures.[10] Radioactivity was measured using an Activimeter ISOMED 2010 (Nuklear-Medizintechnik, Dresden, Germany). For accurate quantification of radioactivity, experimental samples were counted for 1 min on a Hidex gamma counter by using a dynamic energy window of 400–600 keV for ^{64}Cu (511 keV emission). Statistical analyses (Student's *t*-test, confidence interval 95%) were performed using Graphpad Prism Version 7.0.

Syntheses

Methyl 2-((4,7-bis(pyridin-2-ylmethyl)-1,4,7-triazonan-1-yl)methyl)thiazole-4-carboxylate (2)

The 1,4-bis(pyridin-2-ylmethyl)-tacn no2py (515 mg, 1.65 mmol) and potassium carbonate (686 mg; 4.96 mmol) were dissolved in 65 mL of CH_3CN.[27–29] Compound (1) (349 mg, 1.82 mmol) in 5 mL of CH_3CN was added and the reaction mixture was stirred at room temperature for 3 days.[30] After filtration through a celite pad, the filtrate was evaporated and the brown residue was purified on alumina column chromatography ($CHCl_3$ to $CHCl_3$/CH_3OH 90/10). Compound (2) was isolated as brown oil (354 mg; 46%). ^{1}H NMR (500 MHz, $CDCl_3$, 298 K) δ (ppm): 8.49 (m, 2H, CH_{ar}), 8.12 (s, 1H, CH), 7.64 (t, 2H, J = 10 Hz, CH_{ar}), 7.49 (m, 2H, CH_{ar}), 7.14 (m, 2H, CH_{ar}), 3.99 (s, 2H, CH_2), 3.92 (s, 4H, CH_2 py), 3.85 (s, 3H, CH_3), 2.95 (m, 12H, CH_2 tacn). ^{13}C NMR (125 MHz, $CDCl_3$, 298 K) δ (ppm): 162.1 (C = O), 149.1 (CH_{ar}),146.4 (C), 136.5, 128.4, 123.5, 122.1 (CH_{ar}), 60.3 (CH_2), 56.3 (CH_2 tacn), 52.5 (CH_3). ESI-HRMS m/z calculated for $[C_{24}H_{31}N_6O_2S + H]^+$ 467.2224, found 467.2231; calculated for $[C_{24}H_{30}N_6O_2S + Na]$ 489.2043, found 489.2048.

2-((4,7-bis(pyridin-2-ylmethyl)-1,4,7-triazonan-1-yl)methyl)thiazole-4-carboxylic acid, Hno2py1tha, nHCl

Compound (2) (254 mg, 0.54 mmol) was dissolved in 10 mL of 6M HCl aqueous solution and the reaction mixture was stirred at reflux for 18 h. After evaporation of the solvent, Hno2py1tha, nHCl was obtained as yellow powder (346 mg, 95% for n = 6). ^{1}H NMR (400 MHz, 298 K, D_2O) δ (ppm): 8.37–8.41 (m, 2H, CH_{ar}), 8.29 (s, 1H, CH), 8.20–8.27 (m, 2H, CH_{ar}), 7.81 (d, 2H, J = 8 Hz, CH_{ar}), 7.64–7.70 (m, 2H, CH_{ar}), 4.64 (s, 2H, CH_2), 4.01 (s, 4H, CH_2), 3.26–3.29 (m, 4H, CH_2 tacn), 2.79–2.81 (m, 4H, CH_2 tacn), 2.57 (s, 4H, CH_2 tacn). ^{13}C NMR (75 MHz, 298 K, D_2O) δ (ppm): 166.2 (C = O), 163.0, 153.9 (C), 150.3 (CH), 149.5 (C), 144.3, 130.6, 129.3 (CH), 58.4, 57.1 (CH_2), 54.7, 52.6, 48.9 (CH_2 tacn). ESI-HRMS m/z calculated for $[C_{23}H_{31}N_6O_2S + H]^+$ 453.2067, found 453.2064; for $[C_{23}H_{28}N_6NaO_2S]^+$ 475.1887, found 475.1880.

Methyl 6-(2-(hydroxymethyl)pyridin-4-yl)hex-5-ynoate (3)

The compounds (4-bromo-2-pyridine)methanol (1.01 g, 5.37 mmol) and methyl-5-hexynoate (980 mg, 7.77 mmol, 1.4 equivalents) was dissolved in 20 mL of THF/NEt_3 mixture (1/1 v/v). The obtained solution was filled with N_2 and freeze-pump-thaw degassed three times. [$Pd(PPh_3)_2$]Cl_2 (114 mg, 0.16 mmol, 0.06 equivalent) and CuI (63 mg, 0.33 mmol, 0.03 equivalent) were added and the obtained black solution was stirred at 55°C overnight. The palladium was filtered through a celite pad and the filtrate was evaporated to dryness. The obtained black oil was taken up in CH_2Cl_2 and the organic phase was washed with NH_4Cl (3 × 30 mL), brine (3 × 30 mL), and NH_4OH (3 × 30 mL). The combined organic phases were dried over $MgSO_4$, evaporated and purified on silica chromatography column (Hex/AcOEt 60/40 to AcOEt 100). Compound (3) was isolated as black oil (927 mg,

75%). ^{1}H NMR (300 MHz, $CDCl_3$, 298 K) δ (ppm): 8.35 (d, 1H, J = 5 Hz, CH_{ar}), 7.25 (s, 1H, CH_{ar}), 7.07 (d, 1H, J = 5 Hz, CH_{ar}), 4.65 (s, 2H, CH_2OH), 3.61 (s, 3H, CH_3 ester), 2.40–2.46 (m, 4H, CH_2), 1.86 (qt, 2H, J = 6 Hz, CH_2). ^{13}C NMR (75 MHz, $CDCl_3$, 298 K) δ (ppm): 173.0 (C=O), 160.3 (C), 148.0 (CH_{ar}), 132.5 (C), 123.9, 122.5 (CH_{ar}), 94.1, 79.0 (C≡C), 64.0 (CH_2), 51.2 (CH_3), 32.4, 23.2, 18.5 (CH_2).

Methyl 6-(2-(((methylsulfonyl)oxy)methyl) pyridin-4-yl)hex-5-ynoate (4)

Compound (3) (465 mg, 1.99 mmol) was dissolved in 36 mL of CH_2Cl_2 and NEt_3 (605 mg, 5.98 mmol, 3 equivalents). A solution of mesyl chloride (345 mg, 3.01 mmol, 1.5 equivalents) in 7 mL of CH_2Cl_2 was added dropwise and the reaction mixture was stirred at room temperature for 4 h. After disappearance of compound (3) confirmed by TLC, the organic layer was washed with saturated $NaHCO_3$ (3 × 40 mL) and brine (3 × 40 mL), and dried over $MgSO_4$. After evaporation of the organic layer, compound (4) was obtained as a red oil (592 mg, 95%). ^{1}H NMR (300 MHz, $CDCl_3$, 298 K) δ (ppm): 8.54 (d, 1H, J = 5 Hz, CH_{ar}), 7.47 (s, 1H, CH_{ar}), 7.29 (d, 1H, J = 5 Hz, CH_{ar}), 5.32 (s, 2H, CH_2OMs), 3.69 (s, 3H, CH_3 ester), 3.12 (s, 3H, CH_3SO_2), 2.47–2.56 (m, 4H, CH_2), 1.95 (qt, 2H, J = 6 Hz, CH_2). ^{13}C NMR (75 MHz, $CDCl_3$, 298 K) δ (ppm): 173.2 (C=O), 153.6 (C), 149.4 (CH_{ar}), 133.2 (C), 125.6, 124.3 (CH_{ar}), 95.4, 78.7 (C≡C), 71.0 (CH_2), 51.5, 37.9 (CH_3), 32.7, 23.4, 18.8 (CH_2).

1,4-bis(pyridin-2-ylmethyl)-7-(methyl-pyridin-4-ylmethyl-hex-5-ynoate)-1,4,7-triaza-cyclononane (5)

Compounds no2py (420 mg, 1.35 mmol) and potassium carbonate (373 mg, 2.70 mmol, 2 equivalents) were dissolved in 55 mL of CH_3CN.[27–29] After 15 min of stirring, a solution of compound (4) (504 mg, 1.62 mmol, 1.2 equivalents) in 7 mL of CH_3CN was added dropwise over a period of 15 min. The reaction mixture was stirred at room temperature for 2 days. After filtration through celite, the filtrate was evaporated and the black residue was purified on alumina chromatography column ($CHCl_3$ to $CHCl_3/CH_3OH$ 99/1). The ester intermediate (5) was isolated as brown oil (380 mg 54%). ^{1}H NMR (300 MHz, CD_3CN, 298 K) δ (ppm): 8.37 (d, 2H, ^{3}J = 6 Hz, CH_{ar}), 8.31 (d, 1H, ^{3}J = 6 Hz, CH_{ar}), 7.56–7.63 (m, 2H, CH_{ar}), 7.41–7.43 (m, 3H, CH_{ar}), 7.04–7.11 (m, 3H, CH_{ar}), 3.69 (s, 4H, CH_2 py), 3.66 (s, 2H, CH_2 py), 3.52 (s, 3H, CH_3 ester), 2.74 (s, 12H, CH_2 tacn), 2.35–2.44 (m, 4H, CH_2), 1.78 (qt, 2H, J = 9 Hz, CH_2). ^{13}C NMR (75 MHz, CD_3CN, 298 K) δ (ppm): 174.2 (C = O), 161.9, 161.5 (C), 149.9, 149.8 (CH_{ar}), 132.9 (C), 137.3, 126.0, 124.8, 124.2, 122.8, (CH_{ar}), 95.1, 80.4 (C≡C), 65.4, 65.1 (CH_2 py), 56.9, 56.8, 56.6 (CH_2 tacn), 52.2 (CH_3), 33.5, 24.6, 19.5 (CH_2). ESI-HRMS m/z calculated for $[C_{31}H_{38}N_6O_2 + H]^+$ 527.3129, found 527.3127.

1,4-bis(pyridin-2-ylmethyl)-7-(methyl-pyridin-4-ylmethyl-hex-5-ynoic acid)-1,4,7-triaza-cyclononane, no3pyCOOK

Compound (5) (100 mg, 0.19 mmol) was dissolved in 20 mL of THF and 2 mL of 1M KOH was added. The reaction mixture was stirred at 55°C overnight. After evaporation of the solvent, the brown residue was purified by G10 Sephadex exclusion chromatography column. The no3pyCOOK was obtained as brown oil (96 mg, 99%). ^{1}H NMR (300 MHz, D_2O, 298 K) δ (ppm): 8.51 (d, 2H, J = 6 Hz, CH_{ar}), 8.38 (d, 1H, J = 6 Hz, CH_{ar}), 7.79 (t, 2H, J = 9 Hz, CH_{ar}), 7.65 (s, 1H, CH_{ar}), 7.35–7.44 (m, 5H, CH_{ar}), 4.01 (s, 4H, CH_2 py), 3.91 (s, 2H, CH_2 py), 2.89 (s, 12H, CH_2 tacn), 2.45 (t, 2H, J = 6 Hz, CH_2), 2.28 (t, 2H, J = 6 Hz, CH_2), 1.81 (qt, 2H, J = 6 Hz, CH_2). ^{13}C NMR (75 MHz, D_2O, 298 K) δ (ppm): 184.9 (C=O), 159.5, 156.6 (C), 151.8, 151.2, 141.1 (CH_{ar}), 136.3 (C),128.9, 128.5, 127.4, 126.8 (CH_{ar}), 100.3, 81.4, (C≡C), 64.2, 63.1 (CH_2 py), 52.1 (CH_2 tacn), 39.5, 27.6, 21.6, (CH_2). ESI-HRMS m/z calculated for $[C_{30}H_{35}N_6O_2 + K]^+$ 551.2531, found 551.2531, $[M + K]^+$; for $[C_{30}H_{35}N_6O_2 + H]^+$ 513.2973, found 513.2972, $[M + H]^+$.

Dimethyl 6,6′-(((7-pyridin-2-ylmethyl)-1,4,7-triazonane-1,4-diyl)bis(methylene))bis(pyridi-ne-2,4-diyl))bis(hex-5-ynoate) (6)

The no1py was taken up in H_2O and the pH was reach to 14 with NaOH pellets. The aqueous layer was extracted with $CHCl_3$ (3 × 30 mL).[36] The combined organic layers were dried over $MgSO_4$, filtered, and evaporated under pressure. The oily residue (431 mg; 1.96 mmol) was dissolved in dry CH_3CN (45 mL) with K_2CO_3 (3.00 g, 19.58 mmol). Then, compound (4) (1.34 g, 4.31 mmol, 2.2 equivalents) was dissolved in CH_3CN (5 mL) and added dropwise to the previous solution. After 24 h at 40°C, the reaction mixture was filtered and the filtrate was evaporated under reduced pressure. The crude brown oil was purified by alumina chromatography column (CH_2Cl_2/CH_3OH 100/0 to 99/1 to 95/5 to 90/10) yielding compound (6) as an orange oil (557 mg, 45%). ^{1}H NMR (300 MHz, CD_3CN, 298 K) δ (ppm): 8.35 (d, 1H, J = 6 Hz, CH_{ar}), 8.26 (d, 2H, ^{3}J = 6 Hz, CH_{ar}), 7.52–7.57 (m, 1H, CH_{ar}), 7.30–7.37 (m, 3H, CH_{ar}), 7.02–7.10 (m, 3H, CH_{ar}), 3.83 (s, 2H, CH_2 py), 3.74 (s, 4H, CH_2 py), 3.44 (s, 2H, CH_2 py), 2.70–2.77 (m, 12H, CH_2 tacn), 2.25–2.33 (m, 8H, J = 6 Hz, CH_2), 1.63–1.72 (qt, 4H, J = 6 Hz, CH_2). ^{13}C NMR (75 MHz, CD_3CN, 298 K) δ (ppm): 174.1 (C=O), 137.6 (C), 150.1, 133.0, 126.1, 125.2, 124.5, 123.5 (CH_{ar}), 95.6, 79.8 (C≡C), 52.0 (CH_3), 33.3, 24.4, 19.2 (CH_2). ESI-HRMS m/z calculated for $[C_{38}H_{46}N_6O_4 + H]^+$ 651.3653, found 651.3646; calculated for $[C_{38}H_{46}N_6O_4 + 2H]^{2+}$ 326.1863, found 326.1868.

Potassium 6,6′-(((7-(pyridin-2-ylmethyl)-1,4,7-triazonane-1,4-diyl)bis(methylene))bis(py-ridine-2,4-diyl))bis(hex-5-ynoate), no3py(COOK)$_2$

Compound (6) (147 mg, 0.23 mmol) was dissolved in THF (15 mL) with 1M KOH (1.5 mL) and left for 9 h at reflux. The solvent was evaporated under reduced pressure. The salts were removed by dialysis and the obtained residue was purified by semi-preparative HPLC. The dimeric ligand no3py(COOK)$_2$ was isolated as brown oil (62.7 mg, 40%). ^{1}H NMR (300 MHz, D_2O, 298 K) δ (ppm): 8.42 (d, 1H, J = 6 Hz, CH_{ar}), 8.39 (d, 2H, J = 6 Hz, CH_{ar}), 7.76–7.82 (m, 3H, CH_{ar}), 7.35–7.43 (m, 4H, CH_{ar}), 4.13 (s, 2H, CH_2 py), 3.91 (d, 4H, CH_2 py), 2.67–3.21 (m, 12H, CH_2 tacn), 2.31 (t, 4H, J = 6 Hz, CH_2), 2.21 (t, 4H, J = 6 Hz, CH_2), 1.69 (qt, 4H, J = 6 Hz, CH_2). ^{13}C NMR (75 MHz, D_2O, 298 K) δ (ppm): 184.9 (C=O), 158.8, 155.4 (C), 151.8, 151.3, 141.0 (CH_{ar}), 136.3 (C), 128.6, 128.4, 127.2, 126.9 (CH_{ar}), 100.2, 81.0 (C≡C), 63.7, 62.8 (CH_2 py), 53.1, 52.8, 51.1 (CH_2 tacn), 39.3, 27.4, 21.4 (CH_2). ESI-HRMS m/z calculated for $[C_{38}H_{46}N_6O_4 + H]^+$ 623.3340, found 622.3334; calculated for $[C_{38}H_{46}N_6O_4 + 2H]^{2+}$ 312.1707, found 312.1710.

Peptide synthesis and bioconjugation

The BBN peptide Ahx-[D-Phe^{6}, Statine^{13}] BBN (6–14) = Ahx-JMV594 (Sta=statine) was prepared by standard Fmoc chemistry using Rink amide resin on a CS Bio CS336X peptide synthesizer according to the manufacturer's protocol. A 4-fold excess of coupling reagent (HATU) and corresponding Fmoc protected amino acids (Iris Biotech GmbH, Germany) was used in each coupling step. Purification of the peptide conjugates were done by semi-preparative RP-HPLC using a Rigol L-3000 HPLC system with manual injection consisting of a L-3245 Quaternary Pump and a

L-3500 UV/vis detector (UV detection at 220 nm) in combination with a 250 × 20 mm VDSpher 100 C-18E column (5 µm). The solvent system was A = H_2O (0.1% TFA) and B = acetonitrile (0.1% TFA). Semi-preparative HPLC gradient was 0–20 min 5–95% B at a flow rate of 5.5 mL min^{-1}. Analytical HPLC was performed either on an Agilent 1260 Infinity II System with a Berthold Technologies Flow star^2 LB 514 radiation detector or Agilent 1260 Infinity System equipped with an Agilent 1200 DAD UV detector and a Raytest Ramona detector in series. A Phenomenex Jupiter Proteo (250 × 4.60 mm) or VDSpher 100 C18-E 250 × 4 mm column were used for analytical HPLC. Gradients for each measurement are given in the Supporting Information.

no2py1tha-Ahx-JMV594

Resin loaded with 0.67 mmol·g^{-1} of peptide (102.7 mg, 0.069 mmol) was put in 3 mL of dry DMF. Then, no2py1tha.nHCl (155 mg, 0.27 mmol), HATU (105 mg, 0.27 mmol), and DIPEA (50 µL) were added and the mixture was shaken for 2 h at room temperature. The resin was washed with DMF (3 × 2 mL) followed by CH_2Cl_2 (3 × 2 mL) and finally by diethylether (3 × 2 mL). After deprotection and cleavage with TFA/H_2O/TIS (95/2.5/2.5; v/v), the crude peptide conjugate was precipitated in ice-cold diethylether, centrifuged, and finally purified by semi-preparative RP-HPLC yield: 11.4 mg, 10%. RP-HPLC (analytical, 256 nm): t_R=6.95 min; ESI-LRMS m/z calculated for $[C_{84}H_{117}N_{21}O_{13}S + 2H]^{2+}$ 831.9, found 831.2.

no3py-Ahx-JMV594

Compounds no3pyCOOK (3.3 mg, 6 µmol), PyBOP (4.36 mg, 8.39 µmol) and HOBt (1.13 mg, 8.39 µmol) were dissolved in 400 µL of DMF. DIPEA (1.08 mg, 8.39 µmol) was added. The mixture was added to the Ahx-JMV594 peptide (11.03 mg, 8.99 µmol) and stirred at room temperature. After 3 h, water (2 mL) was added to the reaction mixture and the crude was purified by semi-preparative RP-HPLC yield: 750 µL, 25%. RP-HPLC (analytical, 220 nm): t_R=20.4 min. ESI-HRMS m/z calculated for $[C_{91}H_{125}N_{21}O_{13} + H]^+$ 1720.9878, found 1720.9848.

no3py-(Ahx-JMV594)$_2$

Resin loaded with 0.67 mmol.g^{-1} of peptide (8.6 mg, 5.8 µmol) was put in 3 mL of dry DMF. Then, no3py(COOK)$_2$ (14.5 mg, 0.023 mmol), HATU (17.6 mg, 0.046 mmol), and DIPEA (32 µL) were added and the mixture was shaken for 2 h at room temperature. The resin was washed with DMF (3 × 2 mL) followed by CH_2Cl_2 (3 × 2 mL) and finally by diethyl ether (3 × 2 mL). After deprotection and cleavage with TFA/H_2O/TIS (95/2.5/2.5; v/v), the crude peptide conjugate was precipitated in ice-cold diethyl ether, centrifuged, and finally purified by semi-preparative RP-HPLC yield: 1.4 mg, 20%. RP-HPLC (analytical, 256 nm): t_R=26.20 and 26.60 min. ESI-LRMS m/z calculated for $[C_{158}H_{220}N_{36}O_{26} + 2H]^{2+}$ 1521.4, found 1521.2.

Preparation of Cu metallopeptides

The Cu(II) metallopeptides were synthesized using 1.5-fold excess of $CuCl_2 \cdot 2\ H_2O$ (0.1 mM in ammonium acetate buffer). The bioconjugate (500 µg, 0.30 µmol) in H_2O (250 µL) was mixed with 250 µL of Cu(II) stock solution containing 1.5 equivalents of the corresponding metal salt ($CuCl_2 \cdot 2\ H_2O$) and heated at 95°C for 5 min. After cooling to room temperature, the conjugate was purified using C_{18} Sep Pak cartridge [preconditioned with EtOH and H_2O (5 mL each)]. After loading, the cartridge was washed with H_2O (2 mL) and the product was eluted using EtOH: H_2O (50:50 v/v; 1 mL). After evaporation of EtOH at ambient temperature, samples were lyophilized to give the final metallopeptides.

[^{nat}Cu-no2py1tha-Ahx-JMV594]

Yield: 462 µg, 99%. RP-HPLC (analytical, 256 nm): t_R=6.89 min; ESI-LRMS m/z calculated for $[CuC_{84}H_{117}N_{21}O_{13}S + H]^{2+}$ 861.4, found 861.5.

[^{nat}Cu-no3py-Ahx-JMV594]

Yield: 488 µg, 99%. RP-HPLC (analytical, 220 nm): t_R=21.33 min. ESI-HRMS m/z calculated for $[CuC_{91}H_{115}N_{21}O_{13}]^{2+}$ 891.4525, found 891.4510.

[^{nat}Cu-no3py-(Ahx-JMV594)$_2$]

Yield: 600 µg, 99%. RP-HPLC (analytical, 256 nm): t_R = 27.0 min; ESI-LRMS m/z calculated for $[CuC_{158}H_{220}N_{36}O_{26} + 3H]^{3+}$ 1035.4, found 1035.2.

^{64}Cu-labeling experiments

Radiolabeling was performed in 0.1 M buffered media (pH 5.5 MES, pH 7.2 HEPES, pH 8.2 NH_4OAc). Stock solutions of the bioconjugate were prepared in H_2O (1 nmol μL^{-1}). For labeling experiments, 5 µL of bioconjugate (1:100 dilution of stock solution in corresponding labeling buffer) were mixed with 119 µL of corresponding buffer. To this solution, 1 µL of [^{64}Cu]$CuCl_2$ in 0.1 M HCl (^{64}Cu stock diluted to an activity concentration of ∼1–2 MBq μL^{-1}) was added to give a final volume of 125 µL and a chelator concentration of 0.4 µM. After brief mixing, samples were either incubated at room temperature or 95°C for 15 min. Analysis was initially performed by analytical RP-HPLC. The RCC was also checked by TLC using silica gel microfiber strips (Agilent, iTLC-SG glass microfiber) and DTPA solution (50 mM, pH 7.4). No differences between the HPLC and TLC analysed samples were observed so that determination was continued by TLC. While the radiocomplexes [^{64}Cu][Cu-no3py-Ahx-JMV594], [^{64}Cu][Cu-no3py-(Ahx-JMV594)$_2$], and [^{64}Cu][Cu-no2py1tha-Ahx-JMV594], remained at the origin ($R_f = 0$), uncomplexed ^{64}Cu (in the form of the corresponding DTPA complex) moved with the solvent front ($R_f = 1$).

Lipophilicity (log$D_{oct/PBS}$) measurements

For log$D_{oct/PBS}$ measurements, 1–2 MBq (∼20 µL) of each ^{64}Cu-labeled conjugate were added to a pre-saturated mixture of phosphate-buffered saline (PBS) pH 7.4 (480 µL) and 1-octanol (500 µL). Samples were shaken for 10 min at room temperature, centrifuged at 21 100 ×g for 5 min and 100 µL of each phase were counted for 1 min on a calibrated Hidex gamma counter by using a dynamic energy window of 400–600 keV for ^{64}Cu (511 keV emission). Experiments were performed in triplicate.

Cell culture

PC-3 cells (ATCC, Manassas, VA, USA) were cultured at 37°C in a 5% CO_2 atmosphere (Dulbecco modified Eagle medium with GlutaMAX containing 10% fetal bovine serum, 1% 10 000 U mL^{-1} penicillin and 10 000 U mL^{-1} streptomycin, 1% sodium-pyruvate 100 mM).

Cell internalization assay

For cell internalization, PC-3 cells were seeded at a density of 10^6 cells per well in 6-well plates and incubated overnight with medium (Dulbecco modified Eagle medium with GlutaMAX containing 10% fetal bovine serum, 1% 10 000 U mL^{-1} penicillin and 10 000 U mL^{-1} streptomycin, 1% sodium-pyruvate 100 mM). After 24 h, the medium was removed and the cells were washed with PBS. Approximately 2.5 pmol of each ^{64}Cu-labeled conjugate (radiolabeled in molar activities of ∼20 MBq/nmol) were added to the cells (in triplicates) to give a final volume of 1.5 mL PBS in each well followed by incubation for 1 h at 37°C, 5% CO_2. To determine nonspecific membrane binding and internalization, excess of RM2 (final concentration 1 μM) was added to selected wells. At each time point, the internalization was stopped by removing the medium and washing the cells twice with ice-cold PBS. To remove the receptor-bound radioligand, an acid wash was carried out twice with a 0.1 M glycine buffer pH 2.8 for 5 min on ice. Finally, cells were solubilized with 1N NaOH. Radioactivity of cell fractions (supernatant, receptor bound, and internalized) was measured by a Hidex gamma counter. Experiments were performed in triplicate.

Supplementary material

Supplementary data are available at *Metallomics* online.

Author contributions

The manuscript was written through contributions of all authors. All authors have given approval to the final version of the manuscript.

Conflicts of interest

The authors have no conflicts of interest to declare.

Data availability

^{1}H, ^{13}C NMR and mass spectra of compounds, analytical HPLC of conjugates and metalloconjugates, radio TLC, radio HPLC of radioconjugates are available in the online supplementary material.

Acknowledgements

R.T. and V.P. acknowledge the Ministère de l'Enseignement Supérieur et de la Recherche and the Région Bretagne for AM PhD financial support, the Centre National de la Recherche Scientifique, and the "Service Commun" of NMR facilities of the University of Brest. They also thank the University of Brest for financial support given for the mobilities of A.M. and A.G. in Germany and I.H. in France.

Funding

Ministère de l'Enseignement Supérieur et de la Recherche, France Région Bretagne, France Centre National de Recherche Scientifique (CNRS) Université de Brest, France.

References

1. E. Boros and A. B. Packard Radioactive Transition Metals for Imaging and Therapy, *Chem. Rev.*, 2019, 119 (2), 870–901.
2. J. Pellico, P. J. Gwayne and R. T. M. de Rosales Radiolabelling of Nanomaterials for Medical Imaging and Therapy, *Chem. Soc. Rev.*, 2021, 50 (5), 3355–3423.
3. N. Herrero Alvarez, D. Bauer, J. Hernandez-Gil and J. S. Lewis. Recent Advances in Radiometals for Combined Imaging and Therapy in Cancer, *ChemMedChem.*, 2021, 16 (19), 2909–2941.
4. O. Keinänen, K. Fung, J. M. Brennen, N. Zia, M. Harris, E. van Dam, C. Biggin, A. Hedt, J. Stoner, P. S. Donnelly, J. S. Lewis and B. M. Zeglis, Harnessing ^{64}Cu/^{67}Cu for a Theranostic Approach to Pretargeted Radioimmunotherapy, *Proc. Natl. Acad. Sci.*, 2020, 117 (45), 28316–28327.
5. M. Rybalov, H. J. K. Ananias, H. D. Hoving, H. G. van der Poel, S. Rosati and I. J. de Jong, PSMA, EpCAM, VEGF and GRPR as Imaging Targets in Locally Recurrent Prostate Cancer after Radiotherapy, *Int. J. Mol. Sci.*, 2014, 15, 6046–6061.
6. A. Anastasi, V. Erspamer and M. Bucci Isolation and Structure of Bombesin and Alytesin, Two Analogous Active Peptides from the Skin of the European Amphibians *Bombina* and *Alytes*, *Experientia*, 1971, 27 (2), 166–167.
7. P. Moreno, I. Ramon-Álvarez, T. W. Moody and R T. Jensen Bombesin Related Peptides/Receptors and Their Promising Therapeutic Roles in Cancer Imaging, Targeting and Treatment, *Expert. Opin. Ther. Targets.*, 2016, 20 (9), 1055–1073.
8. R. Cescato, T. Maina, B. Nock, A. Nikolopoulou, D. Charalambidis, V. Piccand and J C. Reubi Bombesin Receptor Antagonists May Be Preferable to Agonists for Tumor Targeting, *J. Nucl. Med.*, 2008, 49 (2), 318–326.
9. M. Llinares, C. Devin, O. Chaloin, J. Azay, A. M. Noel-Artis, N. Bernad, J. A. Fehrentz and J. Martinez Syntheses and Biological Activities of Potent Bombesin Receptor Antagonists, *J. Pept. Res.*, 1999, 53 (3), 275–283.
10. R. Mansi, X. Wang, F. Forrer, S. Kneifel, M. L. Tamma, B. Waser, R. Cescato, J. C. Reubi and H R. Maecke Evaluation of a 1,4,7,10-Tetraazacyclododecane-1,4,7,10-Tetraacetic Acid—Conjugated Bombesin-Based Radioantagonist for the Labeling with Single-Photon Emission Computed Tomography, Positron Emission Tomography, and Therapeutic Radionuclides, *Clin. Cancer. Res.*, 2009, 15 (16), 5240–5249.
11. R. Haag Multivalency as a Chemical Organization and Action Principle, *Beilstein. J. Org. Chem.*, 2015, 11, 848–849.
12. S. Liese and R. Netz Influence of Length and Flexibility of Spacers on the Binding Affinity of Divalent Ligands, *Beilstein J. Org. Chem.*, 2015, 11, 804–816.
13. H. L. Handl, J. Vagner, H. Han, E. Mash, V. J. Hruby and R J. Gillies Hitting Multiple Targets with Multimeric Ligands *Expert. Opin. Ther. Targets.*, 2004, 8 (6), 565–586.
14. S. L. Gawlak, P. A. Kiener, G. R. Braslawsky and R S. Greenfield Homodimeric Forms of Bombesin Act as Potent Antagonists of Bombesin on Swiss 3T3 Cells, *Growth Factors*, 1991, 5 (2), 159–170.
15. M. D. Carrithers and M R. Lerner Synthesis and Characterization of Bivalent Peptide Ligands Targeted to G-Protein-Coupled Receptors, *Chem. Biol.*, 1996, 3 (7), 537–542.
16. K. Abiraj, H. Jaccard, M. Kretzchmar, L. Helm and H R. Maecke Novel DOTA-Based Prochelator for Divalent Peptide Vectorization: Synthesis of Dimeric Bombesin Analogues for Multimodality Tumor Imaging and Therapy, *Chem. Commun.*, 2008, 28 (28), 3248–3250.
17. P. Fournier, V. Dumulon-Perreault, S. Ait-Mohand, R. Langlois, F. Bénard, R. Lecomte and B. Guérin Comparative Study of

64Cu/NOTA-[D-Tyr^{6}, βAla^{11}, Thi^{13}, Nle^{14}] BBN (6-14) Monomer and Dimers for Prostate Cancer PET Imaging, *EJNMMI Res.*, 2012, 2,(1), 8.

18. C. Liolios, B. Buchmuller, U. Bauder-Wüst, M. Schäfer, K. Leotta, U. Haberkorn, M. Eder and K. Kopka Monomeric and Dimeric ^{68}Ga-Labeled Bombesin Analogues for Positron Emission Tomography (PET) Imaging of Tumors Expressing Gastrin-Releasing Peptide Receptors (GRPrs), *J. Med. Chem.*, 2018, 61 (5), 2062–2074.
19. R. Mansi, X. Wang, F. Forrer, B. Waser, R. Cescato, K. Graham, S. Borkowski, J. C. Reubi and H R. Maecke Development of a Potent DOTA-Conjugated Bombesin Antagonist for Targeting GRPr-Positive Tumours, *Eur. J. Nucl. Med. Mol. Imaging.*, 2011, 38 (1), 97–107.
20. R. Mansi, R. Minamimoto, H. Mäcke and A. H. Iagaru. Bombesin-Targeted PET of Prostate Cancer, *J. Nucl. Med.*, 2016, 57 (Supplement 3), 67S–72S.
21. A. Roivainen, E. Kähkönen, P. Luoto, S. Borkowski, B. Hofmann, I. Jambor, K. Lehtiö, T. Rantala, A. Rottmann, H. Sipilä, R. Sparks, S. Suilamo, T. Tolvanen, R. Valencia and H. Minn Plasma Pharmacokinetics, Whole-Body Distribution, Metabolism, and Radiation Dosimetry of ^{68}Ga Bombesin Antagonist BAY 86-7548 in Healthy Men. *J. Nucl. Med.* 2013, 54 (6), 867–872.
22. E. Gourni, L. Del Pozzo, E. Kheirallah, C. Smerling, B. Waser, J. C. Reubi, B. M. Paterson, P. S. Donnelly, P. T. Meyer and H R. Maecke Copper-64 Labeled Macrobicyclic Sarcophagine Coupled to a GRP Receptor Antagonist Shows Great Promise for PET Imaging of Prostate Cancer, *Mol. Pharmaceutics.*, 2015, 12 (8), 2781–2790.
23. G. Makris, A. Shegani, P. H. A. Kankanamalage, M. Kuchuk, R. P. Bandari, C. J. Smith and H M. Hennkens Preclinical Evaluation of Novel ^{64}Cu-Labeled Gastrin-Releasing Peptide Receptor Bioconjugates for PET Imaging of Prostate Cancer, *Bioconjugate. Chem.*, 2021, 32 (7), 1290–1297.
24. A. Guillou, L. M. P. Lima, M. Roger, D. Esteban-Gómez, R. Delgado, C. Platas-Iglesias, V. Patinec and R. Tripier. Tacn-Based Bifunctional Picolinate Ligands for an Efficient Copper Complexation, *Eur. J. Inorg. Chem.*, 2017, 2435–2443.
25. A. Guillou, L. M. P. Lima, D. Esteban-Gómez, R. Delgado, C. Platas-Iglesias, V. Patinec and R. Tripier Endo- versus Exo-cyclic Coordination in Copper Complexes with Methylthiazolylcarboxylate Tacn Derivatives, *Dalton. Trans.*, 2019, 48 (24), 8740–8755.
26. A. Guillou, L. M. P. Lima, D. Esteban-Gómez, N. Le Poul, M. D. Bartholomä, R. Delgado, C. Platas-Iglesias, V. Patinec and R. Tripier. Methylthiazolyl Tacn Ligands for Copper Complexation and their BCA Derivatives for Bioconjugation and ^{64}Cu radiolabeling: an Example with Bombesin, *Inorg. Chem.*, 2019, 58 (4), 2669–2685.
27. M. Roger, L. M. P. Lima, M. Frindel, C. Platas-Iglesias, J. F. Gestin, R. Delgado, V. Patinec and R. Tripier Monopicolinate-Dipicolyl Derivative of Triazacyclononane for Stable Complexation of Cu^{2+} and $^{64}Cu^{2+}$, *Inorg. Chem.*, 2013, 52 (9), 5246–5259.
28. G. Gasser, L. Tjioe, B. Graham, M. J. Belousoff, S. Juran, M. Walther, J. U. Künstler, R. Bergmann, H. Stephan and L. Spiccia Synthesis, Copper(II) Complexation, ^{64}Cu-Labeling, and Bioconjugation of a New Bis(2-pyridylmethyl) Derivative of 1,4,7-Triazacyclononane, *Bioconjugate. Chem.*, 2008;19 (3), 719–730.
29. V. Stavila, M. Allali, L. Canaple, Y. Storzt, C. Franc, P. Maurin, O. Beuf, O. Dufay, J. Samarut, M. Janier and J. Hasserodt Significant Relaxivity Gap between a Low-Spin and a High-Spin Iron(II) Complex of Structural Similarity: an attractive Off—On System for the Potential Design of Responsive MRI Probes. *New J. Chem.*, 2008, 32 (3), 428.
30. A. Aditya and T. Kodadek Incorporation of Heterocycles into the Backbone of Peptoids to Generate Diverse Peptoid-Inspired One Bead One Compound Libraries, *ACS Comb. Sci.*, 2012, 14 (3), 164–169.
31. M. Studer and C F. Meares Synthesis of novel 1, 4, 7-Triazacyclononane-N, N', N"-Triacetic Acid Derivatives Suitable for Protein Labeling. *Bioconjugate Chem.*, 1992, 3, 337–341.
32. P. Désogère, Y. Rousselin, S. Poty, C. Bernhard, C. Goze, F. Boschetti and F. Denat Efficient Synthesis of 1,4,7-Triazacyclononane and 1,4,7-Triazacyclononane-Based Bifunctional Chelators for Bioconjugation: Triazacyclononane-Based Bifunctional Chelators, *Eur. J. Org. Chem*, 2014, 2014 (35), 7831–7838.
33. M. Moreau, S. Poty, J. M. Vrigneaud, P. Walker, M. Guillemin, O. Raguin, A. Oudot, C. Bernhard, C. Goze, F. Boschetti, B. Collin, F. Brunotte and F. Denat. MANOTA: a Promising Bifunctional Chelating Agent for Copper-64 ImmunoPET, *Dalton Trans.*, 2017, 46 (42),14659–14668.
34. H. S. Chong, X. Ma, T. Le, B. Kwamena, D. E. Milenic, E. D. Brady, H. A. Song and M W. Brechbiel Rational Design and Generation of a Bimodal Bifunctional Ligand for Antibody-Targeted Radiation Cancer Therapy, *J. Med. Chem.*, 2008, 51 (1), 118–125.
35. H. S. Chong, H. A. Song, C. S. Kang, T. Le, X. Sun, M. Dadwal, H. Lee, X. Lan, Y. Chen and A. Dai A Highly Effective Bifunctional Ligand for Radioimmunotherapy Applications, *Chem. Commun.*, 2011, 47 (19), 5584–5586.
36. M. Roger, V. Patinec, M. Bourgeois, R. Tripier, S. Triki and H. Handel *Exo* Diastereoisomer of 10-Aryl-1,4,7-Triazabicyclo[5.2.1]Decane as Intermediary in Specific Derivatisation of Triazacyclononane, *Tetrahedron*, 2012, 68 (27–28), 5637–5643.
37. M. Fani, G. P. Nicolas and D. Wild Somatostatin Receptor Antagonists for Imaging and Therapy, *J. Nucl. Med.*, 2017, 58, (Supplement 2), 61S–66S.
38. E. Gourni, R. Mansi, M. Jamous, B. Waser, C. Smerling, A. Burian, F. Buchegger, J. C. Reubi and H R. Maecke N-Terminal Modifications Improve the Receptor Affinity and Pharmacokinetics of Radiolabeled Peptidic Gastrin-Releasing Peptide Receptor Antagonists: Examples of ^{68}Ga- and ^{64}Cu-Labeled Peptides for PET Imaging, *J. Nucl. Med.*, 2014, 55 (10), 1719–1725.
39. R. Delgado and F. da Silva Metal Complexes of Cyclic Tetra-Azatetra-Acetic Acids, *Talanta*, 1982, 29 (10), 815–822.
40. R. Delgado, F. da Silva and M. Vaz The Thermodynamics of Complex Formation of Cyclic Tetra-Aza-Tetracetic Acids, *Inorg. Chim. Acta.*, 1984, 90 (3), 185–190.
41. D. W. McCarthy, R. E. Shefer, R. E. Klinkowstein, L. A. Bass, W. H. Margeneau, C. S. Cutter, C. J. Anderson and M J. Welch Efficient Production of High Specific Activity 64Cu Using a Biomedical Cyclotron, *Nucl. Med. Biol.*, 1997, 24 (1), 35–43.